Synthesis and characterization of low bandgap conjugated donor–acceptor polymers for polymer:PCBM solar cells†

Guoli Tu,‡§[a] Sylvain Massip,‡[b] Philipp M. Oberhumer,‡[b] Ximin He,[a] Richard H. Friend,[b] Neil C. Greenham[b] and Wilhelm T. S. Huck*[a]

Received 28th May 2010, Accepted 3rd August 2010
DOI: 10.1039/c0jm01641a

We report on the synthesis, characterization and photovoltaic performance of three novel semiconducting polymers based on poly[bis-*N*,*N*′-(4-octylphenyl)-bis-*N*,*N*′-phenyl-1,4-phenylenediamine-*alt*-5,5′-4′,7′,-di-2-thienyl-2′,1′,3′-benzothiadiazole]. They differ only in the presence and position of hexyl side-chains on the thienyl groups. **T8TBT-0** has no such side-chains, they face towards the benzothiadiazole in **T8TBT-in** and away in **T8TBT-out**. Based on electron-donating triarylamine and electron-accepting dithienyl-benzothiadiazole groups, the new polymers exhibit low bandgaps and enhanced absorption in the red part of the visible spectrum. Despite their identical backbone they differ in their synthesis and photophysics: **T8TBT-0** and **T8TBT-in** can be synthesized by direct Suzuki coupling but a new synthesis procedure is necessary for **T8TBT-out**. In absorption and luminescence a blue shift is induced by the inward facing, and to a lesser extent by the outward-facing side-chains. From comparison of the photophysics in solutions and films, we conclude that the addition of side-chains reduces formation of aggregates in films and that this effect is stronger for inward-facing side-chains. By blending the three polymers with PCBM in a standard photovoltaic device architecture, **T8TBT-0** performs best with a power conversion efficiency (PCE) of 1.0% (under AM1.5G illumination at 100 mW cm^{-2}) compared to 0.17% and 0.27% for **T8TBT-out** and **T8TBT-in**, respectively.

1. Introduction

Driven by the urgent need for a next-generation low-cost, clean energy source, polymer photovoltaic technologies, especially the blended bulk-heterojunction (BHJ) approach, have been developed extensively since the mid-1990s.[1,2] A large effort has been made to understand and improve the performance of this class of devices, and significant advances in the performance of polythiophene-based photovoltaic devices have been achieved during the past few years.[3–7] The chemical structures of polythiophenes, for example their different side-chains, regioregularities and molecular weights are crucial for phase separation in the active layer and to solar cell performance in general.[3,8–12] A polythiophene, poly(3-hexylthiophene) (P3HT), has long been successfully used as a donor polymer, although plenty of new materials have been reported.

According to the calculated optimum bandgap when utilizing fullerenes as an acceptor, a polymer with a bandgap between 1.5 and 1.7 eV, lower than that of P3HT (1.9 eV), is regarded as ideal for polymer–fullerene BHJ solar cells.[13,14] Therefore, a low-bandgap hole-transporting polymer with absorption edge extended into the near-infrared region is desirable to enhance PCE. A popular design of low-bandgap materials is that of copolymers whose backbone consists of alternating electron-rich (electron donating) and electron-deficient (electron accepting) units. This yields internal donor–acceptor structures, with advantages of tunable optical, electrochemical and electronic properties. Recently, many polymers based on thienyl-benzothiadiazole (-TBT) have been synthesized, using mostly fluorene or carbazole derivatives as the donor unit.[15–25]

Since the initial reports of low bandgap polymer–fullerene[18,26–29] photovoltaic devices, the efficiencies have been dramatically increased.[15–18,30–39] Power conversion efficiencies (PCE) have recently reached 5–7% with several low bandgap polymers blended with (6,6)-phenyl-$C_{[61]}$-butyric acid (PCBM) or (6,6)-phenyl-$C_{[71]}$-butyric acid ($PC_{[71]}BM$) as the acceptor.[4,7,16,30,38,40] The most important reasons for these improvements originate from the material properties: carefully tuned bandgap, improved solubility and higher charge mobility. Blouin *et al.* optimized the energy level of the lowest unoccupied orbital (LUMO) of poly(2,7-carbazole) derivatives by using different electron-withdrawing co-monomers and recently achieved a PCE of 6%.[4,17] Recently, several groups reported a large improvement in the efficiency of a polyfluorene-thiobenzothiadiazole polymer blended with PCBM by side-chain modification.[18–20,31,41]

In order to further improve the efficiency of organic solar cells, it is necessary to have a deep understanding of the relationship between the polymer structure and their corresponding physical properties, especially of the influence of side-chains on device performance. Whereas the influence of side-chain length has been studied,[42–45] there are not many reports on the influence of side-chain position on photovoltaic performance.[20,46]

[a]*Melville Laboratory for Polymer Synthesis, Department of Chemistry, University of Cambridge, Lensfield Road, Cambridge, CB2 1EW, UK. E-mail: wtsh2@cam.ac.uk; Fax: +44 1223 334866; Tel: +44 1223 334370*
[b]*Cavendish Laboratory, Department of Physics, University of Cambridge, J J Thomson Ave., Cambridge, CB3 0HE, UK*

† Electronic supplementary information (ESI) available: Blend morphology, and light absorption in devices. See DOI: 10.1039/c0jm01641a

‡ These authors contributed equally.

§ *Present address*: Wuhan National Laboratory for Optoelectronics, Huazhong University of Science and Technology, Luoyu Road, Wuhan, 430074, China.

In this study, three low-bandgap polymers with bis-*N*,*N*′-(4-octylphenyl)-bis-*N*,*N*′-phenyl-1,4-phenylenediamine as one building block and one of three TBT (5,5-(4,7-di-2′-thienyl-2,1,3-benzothiadiazole) derivatives as the other building block were synthesized. The polymers have the same backbone but differently positioned hexyl side-chains on the thiophene rings in the TBT unit (Scheme 1).

Thus, two aims were pursued: first, we replace the usual electron-donor fluorene derivative by a triarylamine group, to lift the energy level of the highest occupied molecular orbital (HOMO) and to reduce the bandgap. Second, keeping the same conjugated backbone, we carry out a systematic study of the effect of the presence and position of the side chains. The three polymers exhibit not only different solubility, but also blue-shifted absorption and emission. Their photoluminescence efficiency (PLQE), bandgap and solar cell performance also change significantly upon attaching hexyl side-chains to different positions on the thiophenes.

2. Results and discussion

2.1. Design, synthesis and characterization

The structure and the synthesis of all three polymers used in this work, poly[bis-*N*,*N*′-(4-octylphenyl)-bis-*N*,*N*′-phenyl-1,4-phenylenediamine-*alt*-5,5′-4′,7′,-di-2-thienyl-2′,1′,3′-benzothiadiazole], (**T8TBT-0**), poly[bis-*N*,*N*′-(4-octylphenyl)-bis-*N*,*N*′-phenyl-1,4-phenylenediamine-*alt*-5,5′-4′,7′,-di-2-(3-hexyl)-thienyl-2′,1′,3′-benzothiadiazole] (**T8TBT-in**) and poly[bis-*N*,*N*′-(4-octylphenyl)-bis-*N*,*N*′-phenyl-1,4-phenylenediamine-*alt*-5,5′-4′,7′,-di-2-(2-hexyl)-thienyl-2′,1′,3′-benzothiadiazole] (**T8TBT-out**) are shown in Scheme 1. In all three T8TBTs, bis-*N*,*N*′-(4-octylphenyl)-bis-*N*,*N*′-phenyl-1,4-phenylenediamine is used as a building block on account of its electron-rich nature and solubilising effect. 5,5-(4,7-Di-2′-thienyl-2,1,3-benzothiadiazole) (TBT-0) and 5,5-(4,7-di-2′-(3-hyxyl)thienyl-2,1,3-benzothiadiazole) (TBT-out) or 5,5-(4,7-di-2′-(2-hexyl)thienyl-2,1,3-benzothiadiazole) (TBT-in) is used as the other block. The monomers used and their synthesis are shown in Scheme 1. Monomer **1** (TBT-0) and monomer **2** (TBT-in) were prepared according to the literature.[32,47] The other two monomers, monomer **3** and monomer **7** were prepared *via* a multistep synthesis (Scheme 2) and carefully purified before use. **T8TBT-0** and **T8TBT-in** can be obtained by Suzuki-coupling (Pd(0) as catalyst) copolymerization of monomer **3** and monomer **1** (or **2**). On the other hand, the reaction between monomer **3** and 5,5-dibromo-(4,7-di-2′-(6-hyxyl)thienyl-2,1,3-benzothiadiazole is not efficient enough to provide a polymer with comparable molecular weight to **T8TBT-0** and **T8TBT-in**. A new synthetic procedure toward **T8TBT-out** was carried out *via* the Suzuki-coupling co-polymerization between monomer **7** and 4,7-di-(4,4,5,5-tetramethyl-1,3,2-dioxaborolane0–2,1,3-benzothiadiazole. All resulting polymers are soluble in common organic solvents, such as chloroform, tetrahydrofuran (THF) and toluene. Their number-average molecular weights (M_n) were determined to be 1.3×10^4, 1.9×10^4, 2.5×10^4 g mol^{-1} for **T8TBT-0**, **T8TBT-out** and **T8TBT-in**, respectively (Table 1).

Table 1 Molecular weights, number of repeat units, polydispersity indices (PDI) and energy levels of the three T8TBTs

Polymer	M_n (10^3 g mol^{-1})	Repeat units	PDI	HOMO (eV)	LUMO (eV)
T8TBT-0	13	13.9	2.1	−4.8	−3.1
T8TBT-out	19	17.2	2.1	−4.8	−3.0
T8TBT-in	25	22.6	1.3	−5.1	−3.0

2.2. Optical properties

The optical properties of the three T8TBTs were investigated through optical absorption and photoluminescence (PL) spectroscopy in very dilute *o*-xylene solution (40 μg mL^{-1}) and in films. All absorption spectra consist of a high-energy and a low-energy peak and are normalized to the height of the high-energy peak.

In solution, a blue-shift of the low-energy absorption peaks is observed from 556 nm (**T8TBT-0**) to 522 nm (**T8TBT-out**) to 492 nm (**T8TBT-in**) (Fig. 1b). In the same order photoluminescence blue-shifts less than absorption from 673 to 658 to 655 nm (Table 2). PLQE values increase from 8 to 16 to 22%. Measured in this very dilute and well dissolved regime, we assume that the big

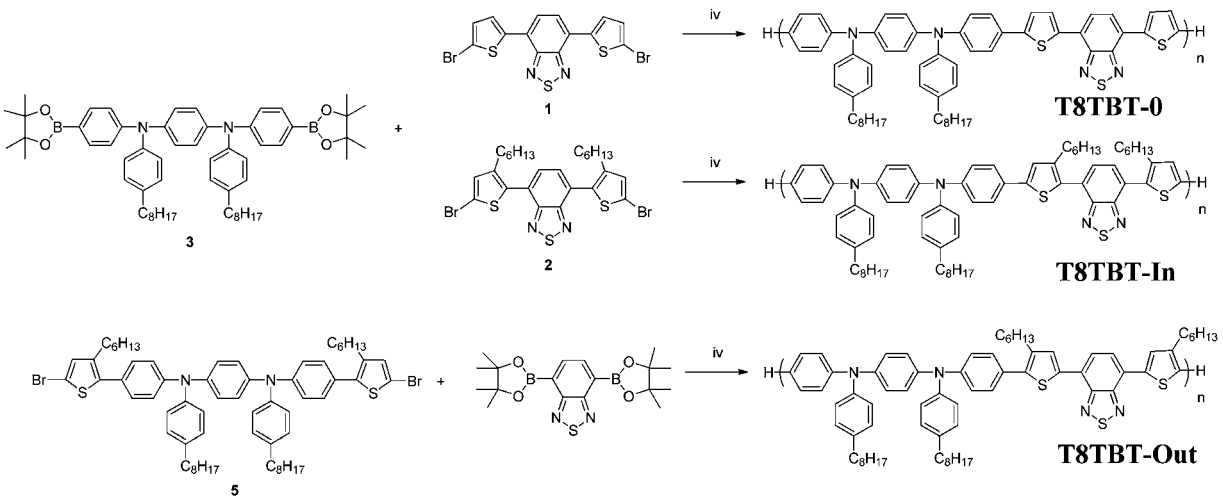

Scheme 1 Synthesis and structures of new TBT-based polymers.

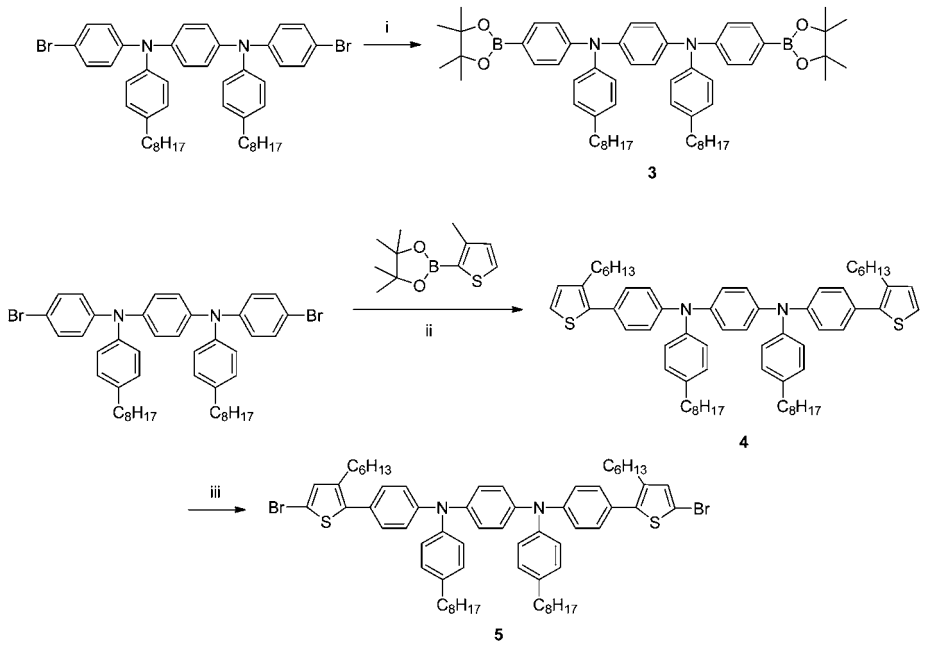

Scheme 2 Synthesis of monomer **3** and **5**.

differences in absorption, photoluminescence spectra and PLQE between the three T8TBTs are caused by their intrinsic intrachain properties. It is likely that the side-chains affect these compounds on the molecular level and have a conformational effect on the chain planarity. Detailed studies of these effects will be published elsewhere.[48]

In films, the optical results follow the same trend: absorption blue shifts from 577 to 541 to 506 nm and also decreases in relative intensity. Stokes shifts of 0.46, 0.52 and 0.62 eV give PL peaks at 725, 700 and 670 nm.

We ascribe all the low-energy absorption peaks (Fig. 1 and 2) to transitions with strong internal charge-transfer character and the high-energy peaks to π–π* transitions as shown for a related donor–acceptor polymer.[21] The low-energy absorption peak is relatively more intense in solution and in films for **T8TBT-0** than **T8TBT-out** and **T8TBT-in**. In films the absorption coefficient α is 110×10^3 cm^{-1}, 81×10^3 cm^{-1}, 58×10^3 cm^{-1}, respectively and will be to some extent affected by a variation in chromophore density.

In the following, we compare, for each polymer, the fluorescence in solution and in film. For **T8TBT-in** the PL peak positions differ by only 0.04 eV (15 nm) and the PLQE is practically the same (22%). On the other hand, for **T8TBT-0** and **T8TBT-out** the PL peaks differ much more by 0.13 eV (52 nm) and 0.11 eV (42 nm). Their PLQEs (film 2%, solution 8% for **T8TBT-0**; film 11% and sol. 16% for **T8TBT-out**) are also more different. This suggests that **T8TBT-0** tends to form exciplexes in films, and that the steric hindrance of the side-chains, especially when facing inwards, increases disorder and prevent the formation of these exciplexes.

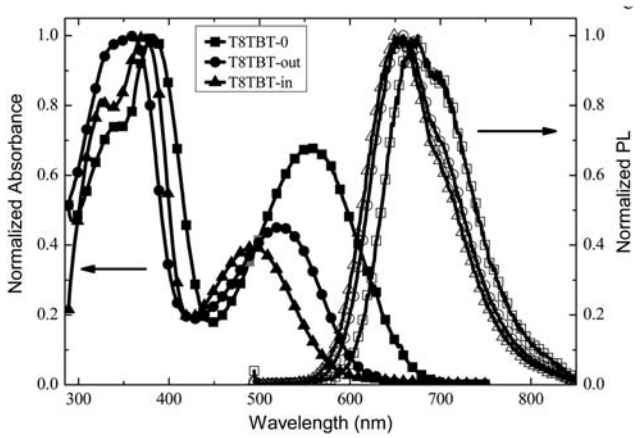

Fig. 1 Normalized absorption (closed symbols) and photoluminescence (open symbols) of **T8TBT-0** (squares), **T8TBT-out** (circles) and **T8TBT-in** (triangles), measured in dilute *o*-xylene solution. For photoluminescence spectra the samples were excited at 488 nm.

2.3. Device performance

The ionization potentials and optical bandgaps of the T8TBTs were estimated respectively from cyclic voltammetry and the onset of optical absorption in order to compare them with other photovoltaic materials. (Table 1) The energy levels thus computed make the T8TBTs suitable for polymer:PCBM BHJ solar cells and such devices were made in the standard architecture (Glass/ITO/PEDOT:PSS/active layer/Al). The best devices were obtained at polymer:PCBM ratios of 1:3. As could have been predicted from the energy levels, the T8TBTs have a rather low and very similar open-circuit voltage under AM1.5G at 1000 W m^{-2} of about 0.6 V (Fig. 3b). This value is similar to what is obtained for P3HT:PCBM blends. Nevertheless the three T8TBTs perform very differently. **T8TBT-0** has a broader absorption spectrum and better external quantum efficiency (EQE) under monochromatic light (Fig. 3a) resulting in a strong increase in

Table 2 Overview of the optical properties of the three T8TBTs in *o*-xylene solutions and in films

Polymer	Absorption peaks, sol (nm)	Absorption peaks, film (nm)	Emission peak, solution (nm)	Emission peak, film (nm)	PLQE in solution (%)	PLQE in film (%)	Stokes shift in solution (eV)	Stokes shift in film (eV)
T8TBT-0	383/557	390/577	673	725	8	2	0.38	0.46
T8TBT-out	357/522	365/541	658	700	16	11	0.49	0.52
T8TBT-in	373/492	375/506	655	670	22	22	0.63	0.62

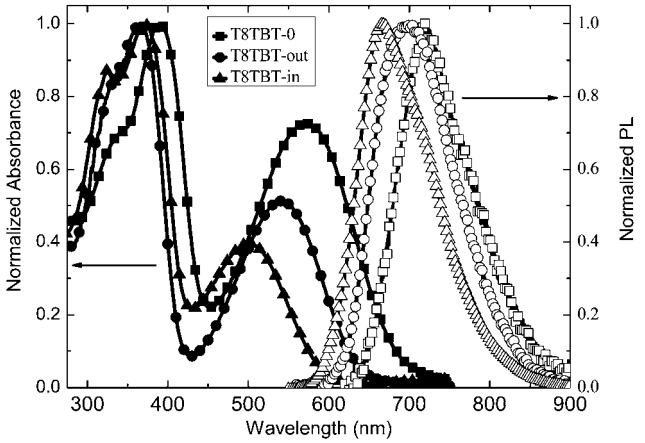

Fig. 2 Normalized absorption (closed symbols) and photoluminescence (open symbols) of **T8TBT-0** (squares), **T8TBT-out** (circles) and **T8TBT-in** (triangles), measured in films spun from chloroform. For photoluminescence the excitation wavelength was 470 nm.

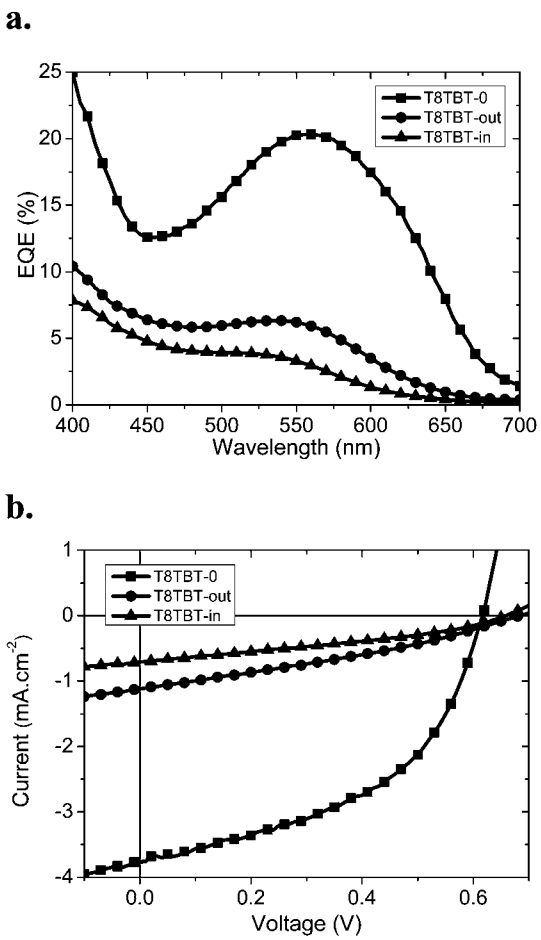

Fig. 3 (a) EQE spectra and (b) *IV* curve under AM1.5G, 100 mW cm^{-2} illumination of optimized T8TBTs:PCBM solar cells. All polymer:-fullerene ratios are 1:3 w/w. **T8TBT-0**:PCBM (squares) were spun from chloroform, **T8TBT-out**:PCBM (circles) and **T8TBT-in**:PCBM (triangles) were spun from chlorobenzene.

short-circuit current under simulated solar conditions. The fill factor of **T8TBT-0** is also better than the T8TBTs with side-chains (Table 3).

T8TBT-0 gives an energy conversion efficiency of 1.0% under AM1.5G spectrum at 1000 W m^{-2} (corrected for the spectral mismatch between the solar simulator and the solar spectrum). The other two T8TBTs with side-chains perform less well in PCBM solar cells. The current best devices have an efficiency of only 0.17% and 0.27% for **T8TBT-in** and **T8TBT-out**, respectively.

The increase in short-circuit current can be partially explained by the larger absorption coefficient of **T8TBT-0** compared with **T8TBT-out** and **T8TBT-in**, but the difference in fill-factor shows that other factors also play a role.

T8TBT:PCBM solar cells were optimized in terms of solvent, active layer thickness, blend ratio and heat treatment. Chloroform was found to be the best solvent for **T8TBT-0** whereas chlorobenzene gave slightly better results for **T8TBT-in** and **T8TBT-out**. The optimal blend ratio was 1:3 w/w polymer to fullerene for all three polymers. 1:4 and 1:5 gave similar results, but 1:2 and 1:1 showed dramatically reduced performance (data not shown). One of the critical parameters for the optimization of these devices was the thickness of the active layer. It turned out that devices worked best with a very thin photoactive layer (60–70 nm), even though the absorbance of the film is much lower than for a thicker film (140 nm) (we estimated the absorbance by measuring the reflectance of real devices in order to account for the interferences in devices,[49] see ESI, S2†). To quantitatively assess this effect in the case of **T8TBT-0** devices, EQEs were measured for devices with active layers of 140 and 70 nm thickness (Fig. 4). The EQE increases from 12% to 19%, which shows that a thinner film is better for charge extraction. This can be explained either by a poor charge transport in the blend or by a need to have a strong internal field to separate the charges.[50]

Charge mobilities are known to affect both charge separation[51] and charge transport.[52] Therefore, the mobilities of the pristine polymers were measured in thin-film transistors (Fig. 5) and give a significantly higher value for **T8TBT-0** (5×10^{-5} cm^2 V^{-1} s^{-1}) than **T8TBT-out** (2×10^{-5} cm^2 V^{-1} s^{-1}) and **T8TBT-in** (4×10^{-6} cm^2 V^{-1} s^{-1}). Generally, higher mobility can be related to better

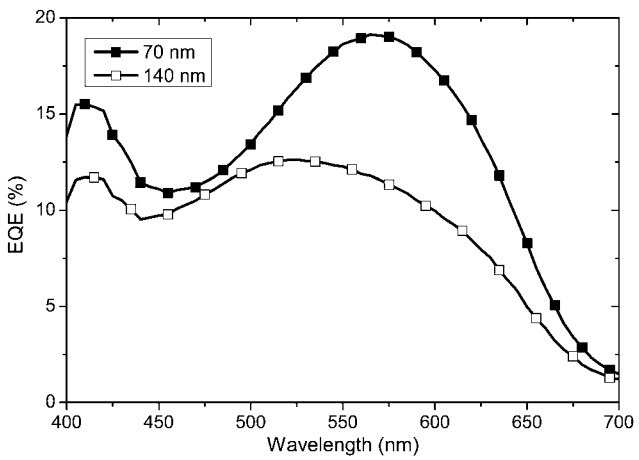

Fig. 4 EQE spectra of **T8TBT-0**:PCBM devices with active layer thicknesses of 140 nm (open squares) and 70 nm (closed squares).

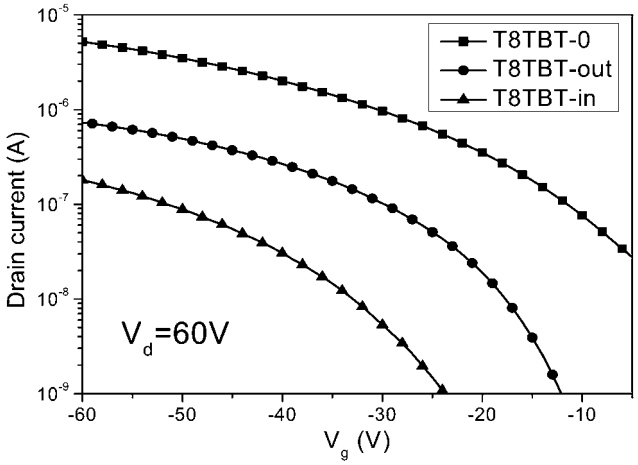

Fig. 5 Transfer characteristics of bottom-gate bottom-contact p-type transistors made of the three T8TBTs. **T8TBT-0** (squares) exhibits a higher mobility than **T8TBT-out** (circles) and **T8TBT-in** (triangles).

π–π stacking,[8] therefore this difference in mobilities correlates well with the difference in chain aggregation that was described above. The mobilities of all three polymers are low, and the highest mobility is found in the best performing material. This indicates that mobilities are probably a crucial parameter in these devices.

Additionally, it is well known that side-chains affect the solubility of polymers, and it has been reported, for example by Troshin *et al.*,[53] that the respective solubilities of the polymer and the fullerene have a strong influence on the blend morphology. It can be argued that the side-chains make the polymers too soluble compared to the fullerene, hence generating a badly performing morphology. Nevertheless, this cannot be verified by atomic force microscopy (AFM): the three polymer:PCBM blends exhibit very similar morphology (see ESI, S1†). It is nevertheless well known that in donor–acceptor polymer:fullerene blends, the PCBM might be too well dispersed into the polymer phase[12,54–56] to be able to resolve the phase separation with AFM and we cannot rule out that the nanostructure changes favorably from **T8TBT-in** to **T8TBT-out** to **T8TBT-0** on a length scale below what can be resolved in the AFM.

3. Conclusions

Three versions of a new semiconducting polymer have been synthesized, varying the side-chains presence and position on the thienyl units: **T8TBT-0**, **T8TBT-out** and **T8TBT-in**. **T8TBT-0** and **T8TBT-in** were synthesised *via* direct Suzuki coupling, whereas a new synthesis procedure was necessary to obtain **T8TBT-out**. The polymers show good solubility, film-forming characteristics and broad absorption, in particular in the red part of the visible spectrum but exhibit very different optoelectronic properties and device performance. The removal of the side-chains causes a strong red-shift both in absorption and photoluminescence emission and decreases significantly the photoluminescence efficiency of the pristine polymer films. In solution, this effect is much smaller and we therefore conclude that side-chain presence and position influence aggregation and intermolecular interactions. Optimised bulk-heterojunction solar cells

using PCBM as an electron acceptor differed significantly in their short-circuit currents and fill-factors and yielded power conversion efficiencies of 0.17%, 0.27% and 1.0% for **T8TBT-in**, **T8TBT-out** and **T8TBT-0**, respectively. These results demonstrate the importance of optimizing the side-chain configuration in low-bandgap conjugated polymers.

4. Experimental

Synthesis, materials and measurements

Compound **1** and **2** were synthesized according to the literature.[32,47] The various chemicals were purchased from Fluka, Aldrich or Acros and used as received.

Bis-*N*,*N*′-(4-octylphenyl)-bis-*N*,*N*′-phenyl-1,4-phenylenediamine (3)

The mixture of 1-(4-bromophenyl) octane (13.5 g, 50 mmol), *N*,*N*′-diphenyl-*p*-phenylenediamine (5.2 g, 20 mmol), sodium *tert*-butyloxide (9.6 g, 0.10 mol), tri-*tert*-butylphosphine (0.101 g, 0.5 mmol), palladium(II) acetate (0.089 g, 0.4 mmol) and toluene (15 mL) was heated to 120 °C under N_2 for 2 days. It was subsequently poured into water and extracted with toluene. The organic layer was washed three times with water and dried with magnesium sulfate. Then the solvent was removed under vacuum. After column chromatography with hexane/toluene (10/1) as an eluant, **4** was obtained as a white solid with a yield of 86%. ^{1}H NMR (benzene, 400 MHz) δ 7.26–7.19 (m, 8H), 7.12 (t, 4H), 7.09 (s, 4H), 7.05 (d, 4H), 6.88 (d, 2H), 2.55 (t, 4H), 1.62 (m, 4H), 1.40–1.25 (m, 20H), 0.95 (t, 6H). ^{13}C (benzene, 400 MHz) δ 148.7, 146.1, 143.4, 137.7, 129.6, 129.4, 125.6, 124.9, 123.6, 122.2, 35.7, 32.2, 32.0, 29.8, 29.7, 29.6, 23.0, 14.3.

Bis-*N*,*N*′-(4-octylphenyl)-bis-*N*,*N*′-(4-bromophenyl)-1,4-phenylenediamine (4)

NBS (4.45g, 25 mmol) in DMF (*N*,*N*′-dimethylformamide, 50 mL) was added into the mixture of compound **7** (6.38 g, 10 mmol) in DMF (50 mL) at 0 °C. The mixture was allowed to warm up to room temperature overnight, poured into water and ice and extracted with toluene. The organic compound was washed three times with water and dried with magnesium sulfate. After removal of the toluene and recrystallisation from ethyl acetate, a white solid was obtained with a yield of 60%. ^{1}H NMR (benzene, 400 MHz) δ 7.21 (d, 4H), 7.12 (d, 4H), 7.07 (d, 4H), 6.98 (s, 4H), 6.89 (d, 4H), 2.55 (t, 4H), 1.62 (m, 4H), 1.40–1.25 (m, 20H), 0.95 (t, 6H). ^{13}C (benzene, 400 MHz) δ 147.5, 145.4, 143.1, 138.4, 132.4, 129.7, 125.5, 125.1, 124.7, 122.2, 114.5, 35.7, 32.2, 31.9, 29.8, 29.7, 29.6, 23.0, 14.3.

Bis-*N*,*N*′-(4-octylphenyl)-bis-*N*,*N*′-(4-(4,4,5,5-tetramethyl-1,3,2-dioxaborolane)phenyl)-1,4-phenylenediamine (5)

BuLi (7 mL, 1.6 M, 11.2 mmol) was added to the mixture of compound **4** (3.97 g, 5 mmol) and THF (40 mL) at −78 °C. Afterwards it was allowed to heat up to room temperature for 10 min and cooled down to −78 °C again and 2-isopropoxy-4,4,5,5-tetramethyl-1,3,2-dioxaborolane (2.5 mL, 12 mmol) was added. After 16 h at room temperature, the reaction was quenched with water; the aqueous phase was extracted with toluene. After washing the organic phase with brine and drying over $MgSO_4$, the toluene was removed under vacuum to obtain a light yellow solid after recrystalization from ethyl acetate (46%). ^{1}H NMR (benzene, 400 MHz) δ 8.15 (d, 4H), 7.28 (d, 4H), 7.19 (d, 4H), 7.07 (s, 4H), 7.02 (d, 4H), 2.53 (t, 4H), 1.62 (m, 4H), 1.31 (m, 20H), 1.20 (s, 24H), 0.95 (t, 6H). ^{13}C (benzene, 400 MHz) δ 151.3, 146.3, 145.5, 143.2, 138.3, 136.6, 129.6, 126.0, 125.6, 124.6, 121.7, 83.4, 35.7, 32.2, 31.9, 29.8, 29.7, 29.6, 24.9, 23.0, 14.3.

Compound 6

$PdCl_2(PPh_3)_2$ (50 mg) was added to a solution of compound **4** (1.368 g, 2 mmol) and 3-hexylthiophene-2-(4,4,5,5-tetramethyl)-1,3,2-dioxaborolane (1,475 g, 5 mmol) in THF (20 mL). The mixture was refluxed in a nitrogen atmosphere for 3 days. After removal of the solvent at a reduced pressure, the residue was purified by column chromatography on silica gel (hexane/toluene = 1/10) to give a yellow solid (yield: 52%).

^{1}H NMR (benzene, 400 MHz) δ 7.44 (d, 4H), 7.28–7.20 (m, 8H), 7.12 (s, 4H), 7.07 (d, 4H), 6.99 (d, 2H), 6.90 (d, 2H), 2.73 (t, 4H), 2.55 (t, 4H), 1.63 (m, 8H), 1.40–1.18 (m, 32H), 0.98 (t, 6H), 0.91 (t, 6H). ^{13}C (benzene, 400 MHz) δ 147.8, 145.7, 143.3, 138.3, 129.7, 129.6, 128.5, 125.8, 125.4, 123.4, 122.7, 35.7, 32.2, 32.0, 31.9, 31.3, 29.8, 29.7, 29.6, 29.4, 29.0, 23.0, 22.9, 14.3, 14.2.

Compound 7

NBS (0.445g, 2.5 mmol) in DMF (15 mL) was added into the mixture of compound **6** (0.858 g, 1.0 mmol) and DMF (10 mL) at 0 °C. The mixture was left at room temperature overnight. After pouring it into water/ice, the mixture was extracted with toluene. The organic layer was washed three times with water and dried with magnesium sulfate. After removal of the toluene and recrystallization from ethyl acetate a yellow solid was obtained with a yield of 57%. ^{1}H NMR (benzene, 400 MHz) δ 7.27 (d, 4H), 7.22 (d, 4H), 7.17 (d, 4H), 7.09 (s, 4H), 7.07 (d, 4H), 6.83 (s, 2H), 2.55 (m, 8H), 1.62 (m, 4H), 1.45 (m, 4H), 1.39–1.14 (m, 32H), 0.95 (t, 6H), 0.91 (t, 6H). ^{13}C (benzene, 400 MHz) δ 148.1, 145.4, 143.2, 139.9, 139.0, 138.6, 132.5, 130.3, 129.8, 127.0, 125.9, 125.7, 122.3, 110.0, 35.7, 32.2, 31.9, 31.8, 31.0, 29.8, 29.7, 29.6, 29.2, 28.8, 23.0, 22.8, 14.3, 14.2.

Polymerizations

Corresponding boronic esters (0.5 mmol) and dibromo monomers (0.5 mmol), 17 mg (0.015 mmol) tetrakis(triphenylphosphine)palladium(0) were dissolved in 5 ml of toluene and 5 ml of 2 M potassium carbonate aqueous solution was added. After reacting under N_2 for three days at 80 °C, the mixture was poured into methanol. The solid was collected and washed/fractionated by Soxhlet extraction with methanol for 24 h and then chloroform. The chloroform fraction was characterized and used.

UV-visible ground state absorption

Films were spun from chloroform and dilute solutions were prepared in *o*-xylene. Samples were measured with an HP8354 spectrometer.

Energy levels

Cyclic voltammetry measurements were carried out on thin films drop-cast from chloroform, with a Gamry reference 600 standard 3-electrode set-up. A wire of platinum was used as the counter-electrode and an Ag/AgCl electrode was used as the reference. Polymer films were dropcast from chloroform onto the working electrode. The electrochemical oxidation potentials were found to be 500 mV, 520 mV and 710 mV against ferrocene for **T8TBT-0**, **T8TBT-out** and **T8TBT-in**, respectively. The HOMO energy levels were estimated from the electrochemical ionisation potential, using 4.8 eV as the HOMO of ferrocene. The LUMO energy level was then estimated by subtracting the bandgap as determined by the onset of optical absorption in eV.

Photoluminescence spectroscopy

PL spectra were recorded with a Varian Cary Eclipse integrated fluorescence spectrophotometer by exciting the samples at 488 nm. Films were spun from chloroform and solutions were prepared with *o*-xylene and measured in 10 mm light-path quartz fluorescence cuvettes. The optical density of these samples was below 0.1 and PLQE values for solutions were calculated directly from the above PL spectra after Lakowicz[57] with Rhodamine 6 G in ethanol as reference.

PLQE in films were computed following de Mello *et al.*[58] by measuring PL spectra inside an integrating sphere with an Oriel Instaspec IV spectrometer. Samples were excited with the 515 nm line of an Argon laser.

Photovoltaic devices

ITO patterned glass substrates were sonicated in acetone and isopropanol for ten minutes each and then etched with an oxygen plasma for ten minutes at 250 W. Immediately afterwards, a 40 nm thick layer of PEDOT:PSS was spun in air and annealed at 170 °C under nitrogen flow. The active layers, blends of T8TBT and PCBM were consequently deposited *via* spin-coating in ambient conditions. Except where otherwise stated, the active layer thickness was 70–80 nm. In the best devices, **T8TBT-0** blends were spun from chloroform and **T8TBT-out** and **T8TBT-in** were spun from chlorobenzene. The devices were then transferred to a glovebox where 100 nm thick aluminium electrodes were deposited through a shadow mask *via* thermal evaporation at a vacuum lower than 10^{-6} mbar. The overlap between the electrodes was 4.5 mm^2. Finally the devices were encapsulated with epoxy glue and a cover glass slide for measurements in air. Devices were illuminated with an Oriel halogen bulb and through a Bentham M300 monochromator at about 1 W m^{-2} for EQE measurements and with an Oriel solar simulator for power conversion efficiency. The spectral mismatch factor is calculated from the solar spectrum, the spectrum of the solar simulator and the low intensity EQE of the device. The intensity of the solar simulator is then tuned so that it corresponds to 1000 W m^{-2} under the solar spectrum AM1.5. Electrical measurements used a Keithley 236 Source Measure Unit.

Table 3 Photovoltaic performance of the best T8TBTs:PCBM blends as active layer. Because of much better fill factor and short-circuit current, **T8TBT-0** performs best. **T8TBT-0**:PCBM (1:3 w/w) were spun from chloroform; T8TBT-out:PCBM (circles) and **T8TBT-in**:PCBM (1:3 w/w) were spun from chlorobenzene

Polymer	V_{oc} (V)	J_{sc} (A m^{-2})	FF	PCE
T8TBT-0	0.62 V	3.8	48%	1.0%
T8TBT-out	0.68 V	1.1	34%	0.27%
T8TBT-in	0.66 V	0.7	32%	0.17%

Mobility values

In order to measure mobility, organic transistors were fabricated. They were measured in bottom-gate, bottom-contact geometry. The contacts were made of gold and the dielectric was SiO_2 covered with a monolayer of octadecyltrichlorosilane (OTS). The drain current was measured in the saturation regime by applying 60 V between the drain and the source and the mobility was extracted by fitting I_d with the standard formula:[59]

$$I_d = \frac{W}{2L}\mu_{sat}C_i\left(V_g - V_{th}\right)^2,$$

where W, the channel width is 10 mm, L, the channel length is 5 μm and C_i, the capacitance per unit area of the dielectric, is 11.5 nF cm^{-2}.

Acknowledgements

The authors thank EPSRC for financial support. SM and PMO thank Sebastian Albert-Seifried, Dr Justin Hodgkiss, Dr Giuseppina Pace and Dr Sven Hüttner for technical help and discussions.

References

1 J. J. M. Halls, C. A. Walsh, N. C. Greenham, E. A. Marseglia, R. H. Friend, S. C. Moratti and A. B. Holmes, *Nature*, 1995.
2 G. Yu, J. Gao, J. C. Hummelen, F. Wudl and A. J. Heeger, *Science*, 1995, **270**, 1789–1791.
3 Y. Kim, S. Cook, S. M. Tuladhar, S. A. Choulis, J. Nelson, J. R. Durrant, D. D. C. Bradley, M. Giles, I. McCulloch, C. Ha and M. Ree, *Nat. Mater.*, 2006, **5**, 197–203.
4 S. H. Park, A. Roy, S. Beaupre, S. Cho, N. Coates, J. S. Moon, D. Moses, M. Leclerc, K. Lee and A. J. Heeger, *Nat. Photonics*, 2009, **3**, 297–302.
5 G. Li, V. Shrotriya, J. Huang, Y. Yao, T. Moriarty, K. Emery and Y. Yang, *Nat. Mater.*, 2005, **4**, 864–868.
6 W. Ma, C. Yang, X. Gong, K. Lee and A. Heeger, *Adv. Funct. Mater.*, 2005, **15**, 1617–1622.
7 H. Chen, J. Hou, S. Zhang, Y. Liang, G. Yang, Y. Yang, L. Yu, Y. Wu and G. Li, *Nat. Photonics*, 2009, **3**, 649–653.
8 H. Sirringhaus, P. J. Brown, R. H. Friend, M. M. Nielsen, K. Bechgaard, B. M. W. Langeveld-Voss, A. J. H. Spiering, R. A. J. Janssen, E. W. Meijer, P. Herwig and D. M. de Leeuw, *Nature*, 1999, **401**, 685–688.
9 P. Schilinsky, U. Asawapirom, U. Scherf, M. Biele and C. J. Brabec, *Chem. Mater.*, 2005, **17**, 2175–2180.
10 R. C. Hiorns, R. de Bettignies, J. Leroy, S. Bailly, M. Firon, C. Sentein, A. Khoukh, H. Preud'homme and C. Dagron-Lartigau, *Adv. Funct. Mater.*, 2006, **16**, 2263–2273.
11 A. M. Ballantyne, L. Chen, J. Dane, T. Hammant, F. M. Braun, M. Heeney, W. Duffy, I. McCulloch, D. D. C. Bradley and J. Nelson, *Adv. Funct. Mater.*, 2008, **18**, 2373–2380.

12 A. C. Mayer, M. F. Toney, S. R. Scully, J. Rivnay, C. J. Brabec, M. Scharber, M. Koppe, M. Heeney, I. McCulloch and M. D. McGehee, *Adv. Funct. Mater.*, 2009, **19**, 1173–1179.
13 M. C. Scharber, D. Mühlbacher, M. Koppe, P. Denk, C. Waldauf, A. Heeger and C. Brabec, *Adv. Mater.*, 2006, **18**, 789–794.
14 C. Soci, I. Hwang, D. Moses, Z. Zhu, D. Waller, R. Gaudiana, C. Brabec and A. Heeger, *Adv. Funct. Mater.*, 2007, **17**, 632–636.
15 N. Blouin, A. Michaud and M. Leclerc, *Adv. Mater.*, 2007, **19**, 2295–2300.
16 E. Wang, L. Wang, L. Lan, C. Luo, W. Zhuang, J. Peng and Y. Cao, *Appl. Phys. Lett.*, 2008, **92**, 033307–3.
17 N. Blouin, A. Michaud, D. Gendron, S. Wakim, E. Blair, R. Neagu-Plesu, M. Belletete, G. Durocher, Y. Tao and M. Leclerc, *J. Am. Chem. Soc.*, 2008, **130**, 732–742.
18 M. Svensson, F. Zhang, S. Veenstra, W. Verhees, J. Hummelen, J. Kroon, O. Inganäs and M. Andersson, *Adv. Mater.*, 2003, **15**, 988–991.
19 M. Chen, J. Hou, Z. Hong, G. Yang, S. Sista, L. Chen and Y. Yang, *Adv. Mater.*, 2009, **21**, 4238–4242.
20 H. Zhou, L. Yang, S. Xiao, S. Liu and W. You, *Macromolecules*, 2010, **43**, 811–820.
21 K. G. Jespersen, W. J. D. Beenken, Y. Zaushitsyn, A. Yartsev, M. Andersson, T. Pullerits and V. Sundstrom, *J. Chem. Phys.*, 2004, **121**, 12613–12617.
22 A. Gadisa, W. Mammo, L. Andersson, S. Admassie, F. Zhang, M. Andersson and O. Inganäs, *Adv. Funct. Mater.*, 2007, **17**, 3836–3842.
23 Q. Zhou, Q. Hou, L. Zheng, X. Deng, G. Yu and Y. Cao, *Appl. Phys. Lett.*, 2004, **84**, 1653–1655.
24 J. Kim, S. H. Kim, I. H. Jung, E. Jeong, Y. Xia, S. Cho, I. Hwang, K. Lee, H. Suh, H. Shim and H. Y. Woo, *J. Mater. Chem.*, 2010, **20**, 1577.
25 L. Biniek, C. L. Chochos, N. Leclerc, G. Hadziioannou, J. K. Kallitsis, R. Bechara, P. Leveque and T. Heiser, *J. Mater. Chem.*, 2009, **19**, 4946–4951.
26 F. Zhang, E. Perzon, X. Wang, W. Mammo, M. Andersson and O. Inganäs, *Adv. Funct. Mater.*, 2005, **15**, 745–750.
27 X. Wang, E. Perzon, F. Oswald, F. Langa, S. Admassie, M. Andersson and O. Inganäs, *Adv. Funct. Mater.*, 2005, **15**, 1665–1670.
28 F. Zhang, K. Jespersen, C. Björström, M. Svensson, M. Andersson, V. Sundström, K. Magnusson, E. Moons, A. Yartsev and O. Inganäs, *Adv. Funct. Mater.*, 2006, **16**, 667–674.
29 F. Zhang, W. Mammo, L. Andersson, S. Admassie, M. Andersson and O. Inganäs, *Adv. Mater.*, 2006, **18**, 2169–2173.
30 J. Peet, J. Y. Kim, N. E. Coates, W. L. Ma, D. Moses, A. J. Heeger and G. C. Bazan, *Nat. Mater.*, 2007, **6**, 497–500.
31 L. H. Slooff, S. C. Veenstra, J. M. Kroon, D. J. D. Moet, J. Sweelssen and M. M. Koetse, *Appl. Phys. Lett.*, 2007, **90**, 143506–3.
32 A. J. Moulé, A. Tsami, T. W. Bünnagel, M. Forster, N. M. Kronenberg, M. Scharber, M. Koppe, M. Morana, C. J. Brabec, K. Meerholz and U. Scherf, *Chem. Mater.*, 2008, **20**, 4045–4050.
33 D. Mühlbacher, M. Scharber, M. Morana, Z. Zhu, D. Waller, R. Gaudiana and C. Brabec, *Adv. Mater.*, 2006, **18**, 2884–2889.
34 A. Tsami, T. W. Bunnagel, T. Farrell, M. Scharber, S. A. Choulis, C. J. Brabec and U. Scherf, *J. Mater. Chem.*, 2007, **17**, 1353–1355.
35 J. Lu, F. Liang, N. Drolet, J. Ding, Y. Tao and R. Movileanu, *Chem. Commun.*, 2008, 5315–5317.
36 M. M. Wienk, M. Turbiez, J. Gilot and R. A. J. Janssen, *Adv. Mater.*, 2008, **20**, 2556–2560.
37 J. Roncali, *Chem. Rev.*, 1997, **97**, 173–206.
38 J. Hou, H. Chen, S. Zhang, R. I. Chen, Y. Yang, Y. Wu and G. Li, *J. Am. Chem. Soc.*, 2009, **131**, 15586–15587.
39 R. Qin, W. Li, C. Li, C. Du, C. Veit, H. Schleiermacher, M. Andersson, Z. Bo, Z. Liu, O. Inganäs, U. Wuerfel and F. Zhang, *J. Am. Chem. Soc.*, 2009, **131**, 14612–14613.
40 L. Huo, J. Hou, S. Zhang, H. Chen and Y. Yang, *Angew. Chem., Int. Ed.*, 2010, **49**, 1500–1503.
41 R. Jadhav, S. Türk, F. Kühnlenz, V. Cimrova, S. Rathgeber, D. A. M. Egbe and H. Hoppe, *Phys. Status Solidi A*, 2009, **206**, 2695–2699.
42 E. Tekin, D. A. M. Egbe, J. M. Kranenburg, C. Ulbricht, S. Rathgeber, E. Birckner, N. Rehmann, K. Meerholz and U. S. Schubert, *Chem. Mater.*, 2008, **20**, 2727–2735.
43 M. C. Iovu, E. E. Sheina, R. R. Gil and R. D. McCullough, *Macromolecules*, 2005, **38**, 8649–8656.
44 D. A. M. Egbe, T. Kietzke, B. Carbonnier, D. Muhlbacher, H. Horhold, D. Neher and T. Pakula, *Macromolecules*, 2004, **37**, 8863–8873.
45 B. Carbonnier, D. A. M. Egbe, E. Birckner, U. Grummt and T. Pakula, *Macromolecules*, 2005, **38**, 7546–7554.
46 E. Wang, M. Wang, L. Wang, C. Duan, J. Zhang, W. Cai, C. He, H. Wu and Y. Cao, *Macromolecules*, 2009, **42**, 4410–4415.
47 Y. Xiao, X. H. Lu, L. W. Tan, K. S. Ong and C. B. He, *J. Polym. Sci. A*, 2009, **47**, 5661–5670.
48 P. M. Oberhumer, Y. Huang, S. Massip, D. T. James, G. Tu, S. Albert-Seifried, J. M. Hodgkiss, J. Kim, W. T. S. Huck, N. C. Greenham, and R. H. Friend, in preparation.
49 A. Moulé and K. Meerholz, *Appl. Phys. B: Lasers Opt.*, 2007, **86**, 721–727.
50 V. D. Mihailetchi, L. J. A. Koster, J. C. Hummelen and P. W. M. Blom, *Phys. Rev. Lett.*, 2004, **93**, 216601.
51 C. Groves, R. A. Marsh and N. C. Greenham, *J. Chem. Phys.*, 2008, **129**, 114903–7.
52 V. D. Mihailetchi, J. Wildeman and P. W. M. Blom, *Phys. Rev. Lett.*, 2005, **94**, 126602.
53 P. A. Troshin, H. Hoppe, J. Renz, M. Egginger, J. Y. Mayorova, A. E. Goryachev, A. S. Peregudov, R. N. Lyubovskaya, G. Gobsch, N. S. Sariciftci and V. F. Razumov, *Adv. Funct. Mater.*, 2009, **19**, 779–788.
54 P. W. M. Blom, V. Mihailetchi, L. Koster and D. Markov, *Adv. Mater.*, 2007, **19**, 1551–1566.
55 J. E. Parmer, A. C. Mayer, B. E. Hardin, S. R. Scully, M. D. McGehee, M. Heeney and I. McCulloch, *Appl. Phys. Lett.*, 2008, **92**, 113309.
56 J. K. Lee, W. L. Ma, C. J. Brabec, J. Yuen, J. S. Moon, J. Y. Kim, K. Lee, G. C. Bazan and A. J. Heeger, *J. Am. Chem. Soc.*, 2008, **130**, 3619–3623.
57 J. R. Lakowicz, *Principles of fluorescence spectroscopy*, Springer, 2006.
58 J. C. D. Mello, H. F. Wittmann and R. H. Friend, *Adv. Mater.*, 1997, **9**, 230–232.
59 J. Zaumseil and H. Sirringhaus, *Chem. Rev.*, 2007, **107**, 1296–1323.

